

25 Predictions of Single-Layer Honeycomb Structures from First Principles

S. Ciraci and S. Cahangirov

25.1 Motivation and Methodology

Finding a contender for graphene in the field of 2D electronics and in other possible potential applications of nanotechnology has derived active search for graphene like novel structures, which do not exist in nature. As a matter of fact, the types of 3D layered materials, which make the exfoliation of their single-layer (SL) structures possible, are limited only to graphite, 2h-BN, 2h-MoS₂, 2h-WSe₂, black phosphorus etc. However, most of desired electronic and magnetic properties demand materials that do not have layered allotropes. In view of the location of C, B, and N elements in the periodic table, which constitute SL graphene and BN, questions have been raised as to whether other group IV elements, group III–V and II–VI compounds may also form SL structures. The theoretical methods have provided for quick answers to guide further experiments. These methods, based on the quantum theory, have now reached now a level of providing accurate predictions for chemical, mechanical, electronic, magnetic, and optical properties of matter.

In our group, we have carried out studies to explore novel materials in SL structure constituted by group IV elements, group III–V and II–VI, group V elements, transition metal oxides, and dichalcogenides, MX₂ in h- and t-structures. We also consider their functionalization by decoration of ad-atoms, by creation of the mesh of vacancies and voids, by formation of nanoribbons or in-plane heterostructures. Most of the elements which construct SL materials have valence orbitals similar to carbon. These are atoms having s² and p^m valence orbitals, which can allow three folded, planar sp² hybrid orbitals to form σ -bonds between two atoms located at the corners of hexagons. This way a three-fold coordinated *honeycomb structure* can be constructed. Remaining p orbitals form bonding (antibonding) π - (π^* -) bonds with nearest neighbors. While the σ -bonds between atoms maintain the mechanical strength, π - π^* -bonds assure the planar geometry and dominate the electronic energy structure near the Fermi level. SL structures including at least one element from the first row of the periodic table, prefer a planar structure such as graphene, h-BN and SiC, since the π -bond is strong enough to maintain the planar geometry. However, the situation is different for SL structures constructed by elements from rows lying below the first one, where nearest-neighbor distance is relatively longer and hence a weaker π -bond cannot maintain the planar geometry. At the end, the structure is stabilized by dehybridization of planar sp²

orbitals, and eventually rehybridization of sp^3 -like orbitals. Accordingly, the structure is buckled, where alternating atoms located at the corners of the hexagon are displaced in opposite and perpendicular directions. In this structural transformation, the projection of atoms continue to form again a honeycomb structure with a 2D hexagonal lattice.

Minimizing the calculated total energy and also atomic forces at each atomic site attains a theoretical prediction of a structure or its functional form. Once the structure optimization resulted in a new SL honeycomb structure, the main issue is whether this structure is stable. Especially, the stability of a structure above room temperature is necessary for technological applications. First, *ab-initio* phonon calculations are carried out to check whether the SL structure remains stable after small displacements of atoms. The structure is viewed as stable when all the frequencies of phonon modes are positive and hence the SL structure corresponds to a local minimum on the Born–Oppenheimer (BO) surface. Imaginary frequencies indicate that the displacements of corresponding modes cannot be restored, and then the structure eventually dissociates. Even if positive phonon frequencies indicate stability, it cannot be assumed that the structure corresponds to a deep local minimum on the BO surface and will remain stable under thermal excitations at high temperature.

The stability at high temperatures is then investigated by performing *ab-initio*, finite temperature molecular dynamics (MD) calculations using two different approaches. Either the Nosè thermostat is used and Newton's equations are integrated through the Verlet algorithm with a time step of 1–2 femtoseconds, or the velocities of atoms were scaled at each time step to keep the temperature constant. MD simulations carried out for several picoseconds at temperatures as high as 1000 K to ensure that the SL structure does not dissociate and hence can remain stable at least above room temperature. Notably, some of the honeycomb structures deduced by the total energy and force calculations were dissociated already at low temperatures after a few time steps, since they were actually unstable.

In addition to phonon frequency and high temperature MD calculations, the stability of optimized structures are subjected to further tests. For example, the possibility that the optimized structure can undergo reconstruction covering several primitive unit cells is tested by optimization in large $n \times n$ supercells. Another possibility that the optimized structure may dissociate or change into clusters is examined by the adsorption of specific ad-atoms or by the formation of defects. Positive cohesive and formation energies are indicative of stability. High mechanical strength suggests robustness. An optimized SL structure, which passes all these stringent tests, is then considered to be stable in the freestanding state even if its parent 3D crystal is not layered like graphite. *It should be noted that the stability of an SL structure does not mean that it can be synthesized; rather it means that this structure remains stable once it is synthesized in freestanding form.* Since certain SL structures can be synthesized only by growing them on specific inert substrates, SL structure–substrate interaction may modify the properties calculated for the freestanding form. Therefore, the properties of the SL structure grown on substrates are calculated to see whether they are affected by the substrate. Single-layer, bilayer, multilayer, and layered periodic structures derived from freestanding SL structures may be stable and display properties gradually

changing with the number of layers. These multilayers can be considered as new polymorphisms of a given SL structure.

The stable SL honeycomb structures are characterized by calculating their equilibrium optimized structural parameters: total energy E_T ; cohesive energy E_C relative to constituent free atoms; formation energy E_f relative to the allotrope having lowest total energy (in the global minimum); elastic, electronic, magnetic, optical properties, etc. In-plane stiffness, $C = A_o^{-1} \partial^2 E_T / \partial \epsilon^2$ (A_o being the equilibrium area of the unit cell) and the Poisson's ratio $\nu = -\epsilon_y / \epsilon_x$ are relevant quantities to quantify the strength and elastic properties of an SL structure. Because of their dimensionality, these structures attain high Poisson ratio and high uniaxial strain under uniaxial stress. In this respect, monitoring of the electronic structure – in particular, of the fundamental band gap with applied strain – is crucial for SL materials. The total charge density $\rho(\mathbf{r})$, charge transfer between constituent atoms are also calculated to provide further information about the character of the binding and bond formation.

The total energies of structures and atomic forces are calculated from the first-principles pseudopotential calculations based on the spin-polarized density functional theory (DFT) using the Vienna *ab-initio* simulation package (VASP) [1]. Since the fundamental band gaps are underestimated by standard DFT, calculations are carried out using the HSE06 hybrid functional [2] and quasi-particle GW_o corrections [3].

25.2 Group IV Elements: Silicene, Germanene

Even before synthesis of isolated graphene, theoretical studies based on the minimization of the total energy have pointed out that the single layer of Si in a buckled honeycomb structure can exist [4, 5]. However, freestanding silicene and germanene, together with their signature of massless Dirac fermion, ambipolar effects and nano-ribbons showing familiar behavior, were first predicted after an extensive stability analysis [6, 7]. The need to unravel the exotic electronic structure and its integrability into the well-established silicon technology has placed silicene at the forefront of intensive theoretical and experimental research. Since Si and Ge do not have any 3D layered allotropes like graphite with weak interlayer van der Waals interaction, silicene cannot be exfoliated and hence freestanding silicene cannot exist in nature.

The stable structure of silicene (germanene) has the following calculated values: the 2D hexagonal lattice constant is $a = 3.83 \text{ \AA}$ (3.97 \AA); the buckling height is $\Delta = 0.44 \text{ \AA}$ (0.64 \AA) [6]. The phonon dispersion curves of silicene and germanene calculated for optimized buckled structures are shown in Fig. 25.1(c). Their stability continues to exist even above room temperature as revealed from *ab-initio* MD calculations performed at 1000 K for 10 picoseconds; similar tests have been done for finite size flakes, indicating stability above room temperature. The electronic energy band structures of silicene and germanene presented in Fig. 25.1(d) show the π - and π^* -bands linearly crossing at the Fermi level. Spin-orbit coupling included later brought about other features such as topological insulator behavior [8]. Not only the physical properties of 2D periodically repeating silicene and germanene are similar to graphene, but also those of their

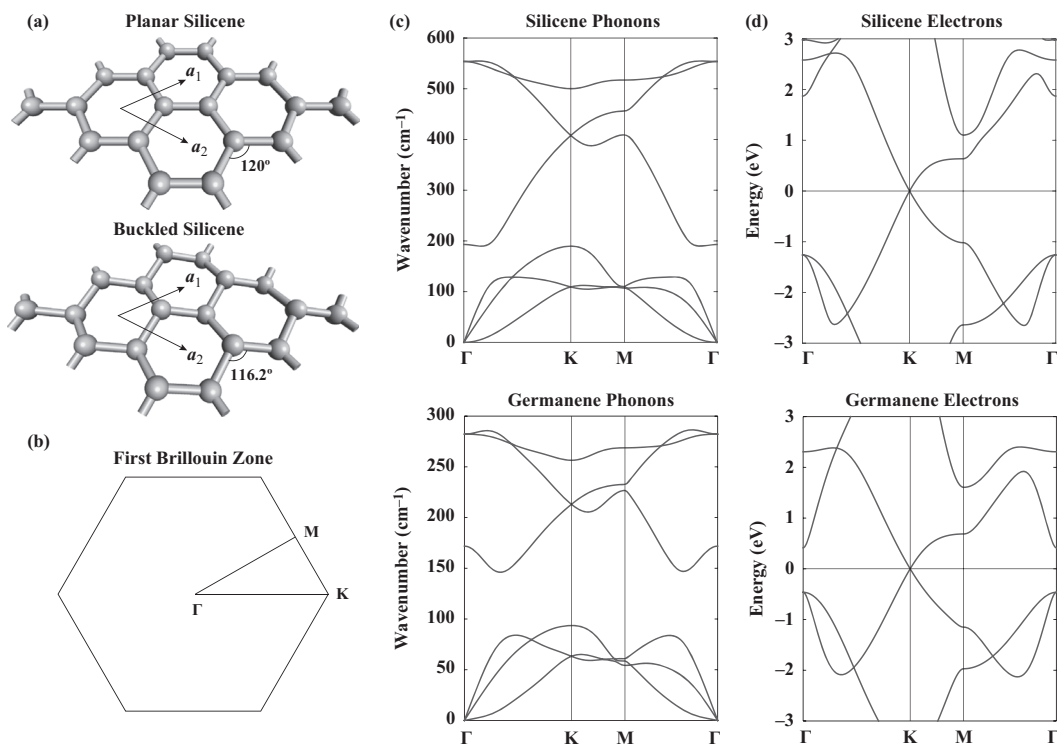


Fig. 25.1 (a) Ball and stick model of planar and buckled silicene. (b) The first Brillouin zone of a honeycomb structure and corresponding symmetry points. (c) Calculated phonon dispersion curves of SL silicene and germanene in optimized, buckled honeycomb structure. (d) Electronic energy band structure of buckled silicene and germanene.

nanoribbons are reminiscent of graphene nanoribbons. For example, the armchair nanoribbons of silicene display the behavior similar to graphene, except that the edge atoms of the former are 2×1 reconstructed [6, 7].

Prediction of SL silicene boosted efforts to grow silicene on a substrate. Silicene was synthesized for the first time on an Ag(111) substrate [9]. It was shown that silicene acquires a 3×3 reconstruction, which is in perfect match with the 4×4 supercell of the Ag(111) surface. Moreover, linear bands near the Fermi level revealed by ARPES performed on the 3×3 silicene grown on Ag(111) are attributed to the significant hybridization between silicene and Ag *sp* bands [10].

The $\sqrt{3} \times \sqrt{3}$ reconstruction is also frequently observed when silicene is deposited on an Ag(111) surface. Here two bright spots are formed in each $\sqrt{3} \times \sqrt{3}$ supercell of silicene, making a honeycomb STM pattern [11, 12]. In contrast to 3×3 and $\sqrt{7} \times \sqrt{7}$ reconstructions, the $\sqrt{3} \times \sqrt{3}$ reconstruction in silicene is not matched by any lattice vector on the Ag(111) surface. Furthermore, it was found that the in-plane lattice constant of $\sqrt{3} \times \sqrt{3}$ silicene is 5% smaller than the corresponding value in freestanding silicene. A model was proposed to explain the spontaneous formation of these 5% contracted $\sqrt{3} \times \sqrt{3}$ silicene structures [13]. According to this model, adding more Si

atoms on top of already formed silicene creates so-called dumbbell units [14, 15]. As the number of dumbbells increase, they organize themselves in such a way that there are two dumbbell units in each $\sqrt{3} \times \sqrt{3}$ supercell. The resulting structure is spontaneously contracted to a lattice constant of 6.4 Å, which is what was measured in the experiments [11,12]. Later it was shown that even more layers with the $\sqrt{3} \times \sqrt{3}$ reconstruction grow as silicon continues to be deposited [16]. Interestingly, the multilayer silicene grown in this fashion was shown to have a metallic character. On the theoretical side, it has been possible to extend the aforementioned $\sqrt{3} \times \sqrt{3}$ dumbbell monolayer of silicene into a layered dumbbell structure called *silicite* [17]. This new allotrope of silicon is only 0.17 eV/atom less favorable than cubic diamond silicon and has an enhanced absorption in the visible range. However, it does not reproduce ~ 3.0 Å interlayer separation observed in multilayer silicene experiments. Recently, multilayer silicene reaching 40 layers was reported [18]. This structure was exposed to ambient air for 24 hours and survived by creating a thin oxide layer on the surface.

More recently, a transistor made of silicene was shown to operate at room temperature [19]. Ambipolar Dirac charge transport with a room temperature mobility of $100 \text{ cm}^2/\text{Vs}$ was measured in this system. Germanene was also synthesized by depositing germanium atoms on an Au(111) substrate [20]. The resulting structure was complex with coexisting phases, one of which was shown to be $\sqrt{3} \times \sqrt{3}$ germanene matched by $\sqrt{7} \times \sqrt{7}$ Au(111). Notably, adsorption of additional Ge ad-atoms on germanene creates dumbbell units such as silicene [21]. Germanene was also synthesized on an Al(111) surface [22]. In this case, the observed structure was uniform consisting of 2×2 germanene matched by a 3×3 Al(111) surface. Finally, stanene was also synthesized by depositing tin atoms on $\text{Bi}_2\text{Te}_3(111)$ surface [23].

25.2.1. Silicon Carbide

Bulk SiC is a material, which is convenient for high temperature and high power devices. One expects that SL SiC can be synthesized, since graphene and silicene are already synthesized, and it may exhibit physical properties which are desired for specific applications in 2D electronics. First-principles calculations have predicted that SL SiC is stable in a honeycomb structure [24]. It is an ionic compound semiconductor with significant charge transfer from the Si to C atom and has a fundamental band gap of $E_G = 2.53$ eV obtained using GGA, which increases to 3.90 eV after G_oW_o corrections. Other relevant properties, i.e. bond length, cohesive energy, and in-plane stiffness, are calculated to be $d = 1.79$ Å, $E_C = 11.94$ eV/per SiC and $C = 166 \text{ J/m}^2$, respectively. When compared with the calculated values of 3D bulk SiC in zincblende or wurtzite structure and 1D chain structures, those of SL SiC in a honeycomb structure display intermediate values, except that the band gap is largest in the SL honeycomb structure [24].

25.2.2 Silicatene

None of the allotropes of silica (i.e. amorphous or crystalline quartz) is known to have a graphite-like layered structure. Despite that, efforts have been devoted to

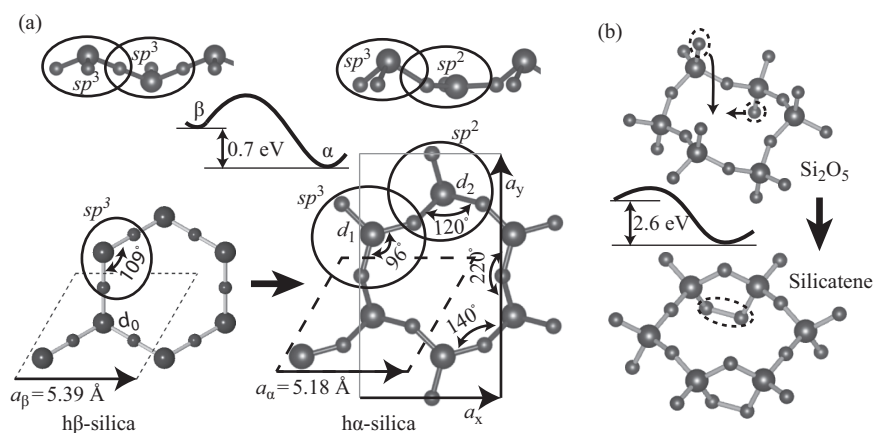


Fig. 25.2 (a) $h\alpha$ -silica derived from $h\beta$ -silica. (b) Silicatene derived from $h\alpha$ -silica (adapted with permission from [26]).

grow a 2D ultra-thin polymorph of silica on substrates [25]. Recently, stable SL allotropes of silica, named as $h\alpha$ -silica and silicatene have been predicted [26]. The optimized structure of $h\alpha$ -silica, which is derived from ideal $h\beta$ -silica by lowering energy by 0.7 eV is described in Fig. 25.2(a). Remarkably, $h\alpha$ -silica is predicted to have a negative Poisson's $\nu = -0.21$. That is, as $h\alpha$ -silica is stretched along the x -direction, it also expands in the y -direction, owing to its squeezed structure consisting of twisted and bent Si—O—Si bonds resulting in a reentrant structure as described in Fig. 25.2(a). The negative Poisson's ratio is a rare situation and those extreme materials having this property are called auxetic or metamaterials. The semiconductor $h\alpha$ -silica is non-magnetic with a direct band gap of 2.2 eV. Moreover, it is a rather rare situation that the variation in the calculated band gap is strain specific; it increases with increasing uniaxial strain ϵ_x , but it decreases with increasing ϵ_y .

Owing to the dangling bonds oozing from Si atoms, $h\alpha$ -silica is rather reactive; through the saturation of Si dangling bonds upon oxidation it transforms to Si_2O_5 and the band gap of $h\alpha$ -silica increases from 2.2 eV to 6 eV, attributing a high insulating character and inertness like 3D silica. While the hexagon-like 2D geometry in Fig. 25.2(a) is maintained, sp^2 bonded Si atoms change to sp^3 bonded Si atoms and hence restore the rotary reflection symmetry. This way, Si atoms acquire the fourfold coordination of oxygen atoms as shown in Fig. 25.2(b) as in 3D silica. Upon heating, Si_2O_5 undergoes a structural transformation by further lowering (i.e. becoming more energetic) its total energy by 2.63 eV. In this transformation, the first half of the dangling Si—O bonds from top to bottom so that all are relocated at the bottom side. Eventually, they are paired to form O—O bonds. The optimized structure predicted in Fig. 25.2(b) replicates the structure of the SL silica in a honeycomb structure named silicatene, the growth of which was achieved recently on a Ru(0001) surface [28].

25.3 Group III–V and II–VI Compounds

Groups III–V and II–VI compound semiconductors in zincblende or wurtzite structures dominate electronics, and optoelectronics. The question whether GaAs can form single wall nanotubes and SL honeycomb structures like graphene was addressed in 2005 [5]. Motivated by these early results, a comprehensive study has been carried out to explore SL structures of group IV elements and group III–V compounds [27]. *Ab-initio* phonon frequency calculations, which resulted in positive frequencies, have demonstrated that 17 new group IV–IV and group III–V compounds can remain stable in a SL honeycomb structure once they are synthesized. The equilibrium structure parameters, cohesive energy, energy band gap, the ratio of effective charges, Poisson's ratio, and in-plane stiffness calculated using LDA approximation are presented in Table 25.1.

Using the calculated values from Table 25.1, interesting correlations between cohesive energy and the lattice constant, and between in-plane stiffness and cohesive energy were deduced as shown in Fig. 25.3. For example, as E_C decreases, the lattice constant a increases with increasing average row number of constituents. Similarly, C and E_C are correlated and both increase with decreasing average row number of constituent elements.

Additionally, the commensurate 1D heterostructures of these materials constructed from their nanoribbons, such as GaN/AlN having multiple quantum well structures with their band-lineups, have been proposed as an extension to 2D SL honeycomb structures [27]. It should be noted that by increasing the widths of nanoribbons and constructing these heterostructures, one can attain in-plane heterostructures or composite structures [29].

25.3.1 Group II–VI Compound: ZnO

Bulk ZnO is an important optoelectronic material, because of its wide band gap of 3.3 eV and large exciton binding energy of 60 meV leading to LED and solar cell applications. Two-monolayer-thick ZnO(0001) films have been grown on an Ag(111) surface [30]. Based on first-principles calculations, an SL ZnO in planar honeycomb structure has been found to be stable [31]. It is a non-magnetic semiconductor and has a lattice constant of $a = 1.89 \text{ \AA}$ and a direct band gap (calculated by GGA and corrected by G_0W_0) $E_G = 5.64 \text{ eV}$. In the bilayer of ZnO, the band gap decreases to 5.10 eV and saturates at 3.32 eV in the graphitic h-ZnO structure. Zig-zag nanoribbons of ZnO are ferromagnetic metals due to spins localized in oxygen atoms at the edges. Whereas bare and H saturated armchair nanoribbons of ZnO are a non-magnetic semiconductor, energy band gap saturates at 1.75 eV as their widths increase.

25.3.2 α -Graphyne and α -BNyne

The stable SL structures α -graphyne and α -BNyne are derived from a honeycomb lattice with additional n atoms between the atoms placed at the corners of hexagon [32]. The

Table 25.1 Calculated values for group IV elements, their binary compounds, and group III–V compounds forming a stable SL honeycomb structure. These are angled between neighboring bonds θ ; buckling parameter Δ ; bond length d ; 2D hexagonal lattice constant a ; cohesive energy E_G ; fundamental band gap E_G calculated by LDA and corrected by GW₀ with symmetry points indicating where the minimum (maximum) of conduction (valence) band occurs; calculated effective charges on the constituent cation/anion Z_c^*/Z_a^* ; Poisson's ratio ν ; in-plane stiffness C (this table is taken with permission from [27]).

GROUP IV										
Material	Geometry	θ (deg)	Δ (Å)	d (Å)	a (Å)	E_C (eV)	E_G (eV) LDA-GW ₀	Z_c^*/Z_a^*	ν	C (J/m ²)
Graphene	Planar	120.0	0.00	1.42	2.46	20.08	Semimetal	0.00/0.0	0.16	335
Silicene	Buckled	116.4	0.44	2.25	3.83	10.32	Semimetal	0.00/0.0	0.30	62
Germanene	Buckled	113.0	0.64	2.38	3.97	8.30	Semimetal	0.00/0.0	0.33	48
SiC	Planar	120.0	0.00	1.77	3.07	15.25	2.52/KM-4.19/KM	1.53/6.47	0.29	166
GeC	Planar	120.0	0.00	1.86	3.22	13.23	2.09/KK-3.83/KK	2.82/5.18	0.33	142
SnGe	Buckled	112.3	0.73	2.57	4.27	8.30	0.23/KK-0.40/KK	3.80/4.20	0.38	35
SiGe	Buckled	114.5	0.55	2.31	3.89	9.62	0.02/KK-0.00/KK	3.66/4.34	0.32	57
SnSi	Buckled	113.3	0.67	2.52	4.21	8.72	0.23/KK-0.68/KK	3.89/4.11	0.37	40
SnC	Planar	120.0	0.00	2.05	3.55	11.63	1.18/TK-6.18/TK	2.85/5.15	0.41	98
GROUP III–V										
Material	Geometry	θ (deg)	Δ (Å)	d (Å)	a (Å)	E_C (eV)	E_G (eV) LDA-GW ₀	Z_c^*/Z_a^*	ν	C (J/m ²)
BN	Planar	120.0	0.00	1.45	2.51	17.65	4.61/KK-6.86/TK	0.85/7.15	0.21	267
AlN	Planar	120.0	0.00	1.79	3.09	14.30	3.08/TK-5.57/TK	0.73/7.27	0.46	116
GaN	Planar	120.0	0.00	1.85	3.20	12.74	2.27/TK-5.00/TK	1.70/6.30	0.48	110
InN	Planar	120.0	0.00	2.06	3.57	10.93	0.62/TK-5.76/TK	1.80/6.20	0.59	67
InP	Buckled	115.8	0.51	2.46	4.17	8.37	1.18/TK-2.88/TK	2.36/5.64	0.43	39
InAs	Buckled	114.1	0.62	2.55	4.28	7.85	0.86/TK-2.07/TK	2.47/5.53	0.43	33
InSb	Buckled	113.2	0.73	2.74	4.57	7.11	0.68/TK-1.84/TK	2.70/5.30	0.43	27
GaAs	Buckled	114.7	0.55	2.36	3.97	8.48	1.29/TK-2.96/TK	2.47/5.53	0.35	48
BP	Planar	120.0	0.00	1.83	3.18	13.26	0.82/KK-1.81/KK	2.49/5.51	0.28	135
Bas	Planar	120.0	0.00	1.93	3.35	11.02	0.71/KK-1.24/KK	2.82/5.18	0.29	119
GaP	Buckled	116.6	0.40	2.25	3.84	8.49	1.92/TK-3.80/KM	2.32/5.68	0.35	59
AlSb	Buckled	114.8	0.60	2.57	4.33	8.04	1.49/KM-2.16/KK	1.58/6.42	0.37	35
BSb	Planar	120.0	0.00	2.12	3.68	10.27	0.39/KK-0.23/KK	3.39/4.61	0.34	91

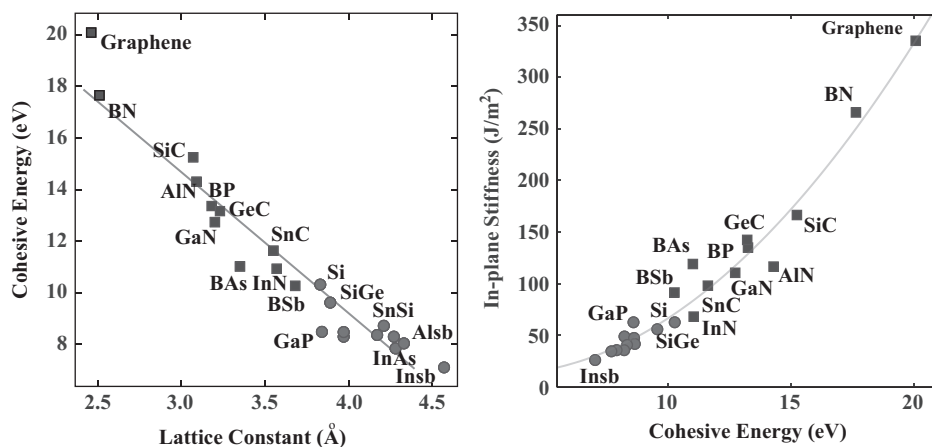


Fig. 25.3 Correlations between the cohesive energy E_C and lattice constant a , and between inplane stiffness C and cohesive energy E_C among stable SL honeycomb structures. Squares and circles are for planar and buckled structures, respectively (adapted with permission from [27]).

SL structure α -graphyne is stable for $n = \text{even}$ and exhibits Dirac cones similar to graphene. However, for $n = \text{odd}$, it is unstable and undergoes a structural transformation by breaking hexagonal symmetry and opening a band gap. The SL structure α -BNyne is a semiconductor with the band gap decreasing with increasing n ; $E_G = 4.13 \text{ eV}$ for $n = 2$, but it decreases to $E_G = 3.46 \text{ eV}$. Both α -graphyne and α -BNyne form stable bilayers with AB stacking.

25.4 Group V Elements: Nitrogene and Antimonene

More recently, the fabrication of a field-effect transistors, using micrometer sized flakes consisting of two to three layers of black phosphorus [33] and theoretical analysis [34], revealing the stability of its single-layer allotropes, i.e. blue and black phospherenes, brought group V elements into focus. Recent theoretical analysis exploring the idea of whether Sb and N can form SL structures have concluded that these two elements can also form stable, SL buckled honeycomb structures, called *nitrogene* and *antimonene*, respectively [35, 36].

Notably, while strong the N_2 molecule is triple bonded, nitrogen is constructed from threefold coordinated and single-bonded N atoms similar to the 3D cg-N crystalline phase. However, unlike semimetallic graphene or silicene which have perfect electron-hole symmetry, nitrogen is a wide band-gap insulator with a DFT band gap of $E_G = 3.96 \text{ eV}$ ($E_G = 5.96 \text{ eV}$ after HSE correction). The buckling distance is $\Delta = 0.7 \text{ \AA}$ and cohesive energy is $E_C = 3.67 \text{ eV/atom}$ [35, 36]. Moreover, nitrogen can form stable nanoribbons with band gaps in the range of $0.6 \text{ eV} < E_G < 2.2 \text{ eV}$, bilayer and 3D graphitic structure named *nitrogenite*.

Antimonene has a stable SL buckled honeycomb (h-Sb) structure, as well as an asymmetric washboard (aW-Sb) structure; the latter has slightly higher cohesive energy.

Here we consider only h-Sb, which has cohesive energy $E_C = 2.87$ eV and is a non-magnetic semiconductor with an indirect band gap of 1.04 eV, calculated within PBE approximation, which occurs between the minimum of the conduction band along the Γ -M direction and a maximum of the valence band at the Γ point. Upon HSE correction the indirect band gap increases to 1.55 eV. Apparently, the band gap of h-Sb lies in the range, which is convenient for several 2D electronic applications. Free-standing SL antimonene is metallized when grown on substrates such as a Ge(111) surface or germanene. Also interlayer coupling is significant and attributes metallicity to bilayer and multilayer antimonene [35, 36].

25.5 Transition Metal Oxides and Dichalcogenides

Three-dimensional transition metal oxides or dichalcogenides MX_2 (M, transition metal; X, oxygen or chalcogen atoms) compounds constitute one of the most interesting classes of crystals; their wide range of properties have been investigated since 1960. Some of these compounds have D_{6h} -point group symmetry and are layered structures formed by the stacking of weakly (vdW) interacting 2D MX_2 layers and are specified as 2h- MX_2 like layered MoS_2 crystals. Another type of layered structure is specified as a 2t-structure (centered honeycomb) and has D_{3d} -point-group symmetry. Some 3D MX_2 structures are known to be stable in rutile, 3R, marcasite, anatase, pyrite, and tetragonal structures.

Interest in 2D materials has led to the synthesis of SL MoS_2 (38), WS_2 (39) with honeycomb structure and NbSe_2 only on SiO_2 . Coleman *et al.* reported liquid exfoliation of MoS_2 , WS_2 , MoSe_2 , TaS_2 , NbS_2 , NiTe_2 , and MoTe_2 (40). In both h and t structures, instead of forming covalent sp^2 -bonding with three neighboring atoms as in graphene, each M atom has the six nearest X atoms and each X atom has the three nearest M atoms forming p-d hybridized ionic M-X bonds. These 2D materials have

Table 25.2 Calculated values of stable, SL, MX_2 in h- and t-structures: Lattice constants, $a = b$; bond lengths, d_{M-X} , d_{X-X} ; X—M—X bond angle, θ ; cohesive energy per MX_2 unit, E_C ; energy band gap, E_G ; total magnetic moment in the unit cell, μ ; in-plane stiffness, C . (The full version of this table can be found in [37]. Reproduced with permission.)

Material	Geometry	a (Å)	d_{M-X} (Å)	d_{X-X} (Å)	θ (deg)	E_C (eV)	E_G (eV)		
							LDA-GW ₀	μ (μ_B)	C (N/m)
MnS_2	t	3.12	2.27	3.29	93.08	14.82	Metal	2.38	66.87
MnSe_2	t	3.27	2.39	3.50	93.78	13.61	Metal	2.35	56.61
MnTe_2	t	3.54	2.59	3.77	93.56	12.27	Metal	2.29	44.77
MoS_2	h	3.11	2.37	3.11	81.62	19.05	1.87–2.57	NM	138.12
MoSe_2	h	3.24	2.50	3.32	83.05	17.47	1.62–2.31	NM	118.37
MoTe_2	h	3.46	2.69	3.59	83.88	15.65	1.25–1.85	NM	92.78
WO_2	h	2.80	2.03	2.45	74.12	24.56	1.37–2.87	NM	250.00
WS_2	h	3.13	2.39	3.13	81.74	20.81	1.98–2.84	NM	151.48
WSe_2	h	3.25	2.51	3.34	83.24	19.07	1.68–2.38	NM	130.04
WTe_2	h	3.47	2.70	3.61	83.96	17.05	1.24–1.85	NM	99.17

shown exceptional physical and chemical properties. For example, transistors fabricated from a SL MoS₂ presented features, which are superior to those of graphene [41]. Also SL MoS₂ appears to be promising for optoelectronic devices, solar cells, LEDs, and HER (hydrogen evaluation reactions).

In an extensive theoretical study exploring other possible SL structures, out of 88 different combinations (M = Sc, Ti, V, Cr, Mn, Fe, Co, Ni, Nb, Mo, W and X = O, S, Se, Te) 52 freestanding, stable h-MX₂ and t-MX₂ structures have been predicted [37]. The optimized lattice constants and values calculated using LDA for selected h-MX₂ and t-MX₂ are presented in Table 25.2.

25.6 Conclusions

Theoretical studies outlined in this chapter predicted 79 new stable, SL honeycomb structures of different elements with electronic and magnetic properties, which may be utilized in the emerging field of nanotechnology. Some of these theoretical predictions have been realized by synthesizing novel SL materials, which are now subjects of active research.

Acknowledgments

Authors acknowledge valuable contributions of their collaborators E. Aktürk, O. Üzengi Aktürk, C. Ataca, E. Durgun, V. O. Özturk, H. Sevinçli, H. Şahin and M. Topsakal to various studies and papers, on which this review is based.

25.7 References

- [1] Kresse G, Furthmüller J. Efficiency of ab-initio total energy calculations for metals and semiconductors using a plane-wave basis set. *Computational Materials Science*. 1996 July, 6(1): 15–50.
- [2] Heyd J, Scuseria GE, Ernzerhof M. Erratum: “Hybrid functionals based on a screened Coulomb potential” [*J. Chem. Phys.* 118, 8207 (2003)]. *The Journal of Chemical Physics*. 2006 June 7, 124(21): 219906.
- [3] Shishkin M, Kresse G. Self-consistent GW calculations for semiconductors and insulators. *Physical Review B*. 2007 June 4, 75(23): 235102.
- [4] Takeda K, Shiraishi K. Theoretical possibility of stage corrugation in Si and Ge analogs of graphite. *Physical Review B*. 1994 November 15, 50(20): 14916–22.
- [5] Durgun E, Tongay S, Ciraci S. Silicon and III–V compound nanotubes: Structural and electronic properties. *Physical Review B*. 2005 August 12, 72(7): 075420.
- [6] Cahangirov S, Topsakal M, Aktürk E, Şahin H, Ciraci S. Two- and one-dimensional honeycomb structures of silicon and germanium. *Physical Review Letters*. 2009 June 12, 102(23): 236804.

- [7] Cahangirov S, Topsakal M, Ciraci S. Armchair nanoribbons of silicon and germanium honeycomb structures. *Physical Review B*. 2010 May 25, 81(19): 195120.
- [8] Ezawa M. A topological insulator and helical zero mode in silicene under an inhomogeneous electric field. *New Journal of Physics*. 2012 March 1, 14(3): 033003.
- [9] Vogt P, De Padova P, Quaresima C, Avila J, Frantzeskakis E, Asensio MC, *et al.* Silicene: Compelling experimental evidence for graphenelike two-dimensional silicon. *Physical Review Letters*. 2012 April 12, 108(15): 155501.
- [10] Cahangirov S, Audiffred M, Tang P, Iacomino A, Duan W, Merino G, *et al.* Electronic structure of silicene on Ag(111): Strong hybridization effects. *Physical Review B*. 2013 July 18, 88(3): 035432.
- [11] Feng B, Ding Z, Meng S, Yao Y, He X, Cheng P, *et al.* Evidence of silicene in honeycomb structures of silicon on Ag(111). *Nanoletters*. 2012 June 4, 12: 3507–11.
- [12] Chen L, Liu C-C, Feng B, He X, Cheng P, Ding Z, *et al.* Evidence for Dirac fermions in a honeycomb lattice based on silicon. *Physical Review Letters*. 2012 August 3, 109(5): 056804.
- [13] Cahangirov S, Özçelik VO, Xian L, Avila J, Cho S, Asensio MC, *et al.* Atomic structure of the 3×3 phase of silicene on Ag(111). *Physical Review B*. 2014 July 28, 90(3): 035448.
- [14] Kaltsas D, Tsetseris L. Stability and electronic properties of ultrathin films of silicon and germanium. *Physical Chemistry Chemical Physics*. 2013, 15(24): 9710–15.
- [15] Özçelik VO, Ciraci S. Local reconstructions of silicene induced by adatoms. *The Journal of Physical Chemistry C*. 2013 December 2, 117: 26305–15.
- [16] Vogt P, Capiod P, Berthe M, Resta A, De Padova P, Bruhn T, *et al.* Synthesis and electrical conductivity of multilayer silicene. *Applied Physics Letters*. 2014 January 13, 104(2): 021602.
- [17] Cahangirov S, Özçelik VO, Rubio A, Ciraci S. Silicite: The layered allotrope of silicon. *Physical Review B*. 2014 August 22, 90(8): 085426.
- [18] De Padova P, Ottaviani C, Quaresima C, Olivieri B. 24 h stability of thick multilayer silicene in air. *2D Materials*. 2014, 1: 021003.
- [19] Tao L, Cinquanta E, Chiappe D, Grazianetti C, Fanciulli M, Dubey M, *et al.* Silicene field-effect transistors operating at room temperature. *Nature Nanotechnology*. 2015 March 1; 10(3):227–31.
- [20] Dávila ME, Xian L, Cahangirov S, Rubio A, Le Lay G. Germanene: A novel two-dimensional germanium allotrope akin to graphene and silicene. *New Journal of Physics*. 2014 September 1, 16(9): 095002.
- [21] Özçelik VO, Kecik D, Durgun E, Ciraci S. Adsorption of group IV elements on graphene, silicene, germanene, and stanene: Dumbbell formation. *The Journal of Physical Chemistry C*. 2014 December 19, 119: 845–53.
- [22] Derivaz M, Dentel D, Stephan R, Hanf M-C, Mehdaoui A, Sonnet P, *et al.* Continuous germanene layer on Al(111). *Nanoletters*. 2015 March 30, 15: 2510–16.
- [23] Zhu F-F, Chen W-J, Xu Y, Gao C-L, Guan D-D, Liu C-H, *et al.* Epitaxial growth of two-dimensional stanene. *Nature Materials*. 2015 October 1, 14(10): 1020–5.
- [24] Bekaroglu E, Topsakal M, Cahangirov S, Ciraci S. First-principles study of defects and adatoms in silicon carbide honeycomb structures. *Physical Review B*. 2010 February 24, 81(7): 075433.
- [25] Shaikhutdinov S, Freund HJ. Ultrathin silica films on metals: The long and winding road to understanding the atomic structure. *Advanced Materials*. 2013 January 4, 25(1): 49–67.

- [26] Özçelik VO, Cahangirov S, Ciraci S. Stable single-layer honeycomblike structure of silica. *Physical Review Letters*. 2014 June 20, 112(24): 246803.
- [27] Şahin H, Cahangirov S, Topsakal M, Bekaroglu E, Aktürk E, Senger RT, *et al.* Monolayer honeycomb structures of group-IV elements and III–V binary compounds: First-principles calculations. *Physical Review B*. 2009 October 28, 80(15): 155453.
- [28] Yang B, Boscoboinik JA, Yu X, Shaikhutdinov S, Freund HJ. Patterned defect structures predicted for graphene are observed on single-layer silica films. *Nanoletters*. 2013 August 14, 13: 4422–7.
- [29] Özçelik VO, Durgun E, Ciraci S. Modulation of electronic properties in laterally and commensurately repeating graphene and boron nitride composite nanostructures. *The Journal of Physical Chemistry C*. 2015 June 2, 119: 13248–56.
- [30] Tusche C, Meyerheim HL, Kirschner J. Observation of depolarized ZnO(0001) monolayers: Formation of unreconstructed planar sheets. *Physical Review Letters*. 2007 July 13, 99(2): 026102.
- [31] Topsakal M, Cahangirov S, Bekaroglu E, Ciraci S. First-principles study of zinc oxide honeycomb structures. *Physical Review B*. 2009 December 11, 80(23): 235119.
- [32] Özçelik VO, Ciraci S. Size dependence in the stabilities and electronic properties of α -graphyne and its boron nitride analogue. *The Journal of Physical Chemistry C*. 2013 January 23, 117: 2175–82.
- [33] Li L, Yu Y, Ye GJ, Ge Q, Ou X, Wu H, *et al.* Black phosphorus field-effect transistors. *Nature Nanotechnology*. 2014 May 1, 9(5): 372–7.
- [34] Zhu Z, Tománek D. Semiconducting layered blue phosphorus: A computational study. *Physical Review Letters*. 2014 May 1, 112(17): 176802.
- [35] Aktürk OÜ, Özçelik VO, Ciraci S. Single-layer crystalline phases of antimony: Antimomenes. *Physical Review B*. 2015 June 25, 91(23): 235446.
- [36] Özçelik VO, Aktürk OÜ, Durgun E, Ciraci S. Prediction of a two-dimensional crystalline structure of nitrogen atoms. *Physical Review B*. 2015 September 15, 92(12): 125420.
- [37] Ataca C, Şahin H, Ciraci S. Stable, single-layer MX_2 transition-metal oxides and dichalcogenides in a honeycomb-like structure. *The Journal of Physical Chemistry C*. 2012 April 16, 116: 8983–99.
- [38] Mak KF, Lee C, Hone J, Shan J, Heinz TF. Atomically thin MoS_2 : A new direct-gap semiconductor. *Physical Review Letters*. 2010 September 24, 105(13): 136805.
- [39] Wang Z, Zhao K, Li H, Liu Z, Shi Z, Lu J, *et al.* Ultra-narrow WS_2 nanoribbons encapsulated in carbon nanotubes. *Journal of Materials Chemistry*. 2011, 21(1): 171–80.
- [40] Coleman JN, Lotya M, O'Neill A, Bergin SD, King PJ, Khan U, *et al.* Two-dimensional nanosheets produced by liquid exfoliation of layered materials. *Science*. 2011 February, 331(6017): 568–71.
- [41] Radisavljevic B, Radenovic A, Brivio J, Giacometti V, Kis A. Single-layer MoS_2 transistors. *Nature Nanotechnology*. 2011 March 1, 6(3): 147–50.